ELSEVIER

Journal of Chromatography A, 845 (1999) 67–83

JOURNAL OF CHROMATOGRAPHY A

Study of the sorption of carbon monoxide, oxygen and carbon dioxide on platinum–rhodium alloy catalysts by a new gas chromatographic methodology

Dimitrios Gavril, George Karaiskakis*

Department of Chemistry, University of Patras, 26500 Patras, Greece

Abstract

The mechanism of the CO oxidation reaction over Pt–Rh alloy catalysts was extracted from the adsorption of CO, O_2 and CO_2 on these catalysts. Reversed-flow gas chromatography was applied to the study of these important sorption processes. Using suitable mathematical analysis, equations were derived by means of which rate constants for the adsorption and desorption of CO, O_2 and CO_2 on and from the Pt–Rh bimetallic catalysts were determined. Temperature dependence of the rate constants for the sorption processes were also determined and the Arrhenius parameters for the adsorption and desorption were calculated. The dependence of activation energies for adsorption, desorption and disproportionation reaction on the catalyst Pt content indicates that for the CO oxidation reaction the most active is the Pt-rich catalyst, while for the CO disproportionation reaction the most active is the Rh-rich catalyst.

Keywords: Catalysts; Platinum–rhodium catalysts; Rhodium–platinum catalysts; Adsorption; Reversed-flow gas chromatography; Carbon monoxide; Carbon dioxide; Oxygen

1. Introduction

Knowledge of the adsorption phenomena on a catalyst is an essential prerequisite to understand the kinetics and mechanism of the catalytic reaction concerned. So long as only static methods of measuring adsorption were available, the catalyst surface could not be studied at high temperatures because the decomposition of the adsorbate by catalytic reaction. However, the surface can be characterized under actual reaction conditions using chromatography, because the flow system reduces the contact time and minimizes decomposition processes. In addition, any small amounts of product formed are separated from the reactant peak by the catalyst acting as a chromatographic stationary phase, and retention measurements relate only to the adsorbing component under study. The features of gas–solid chromatography which makes it suitable for studying catalytic surfaces at high temperature are therefore principally minimal decomposition due to low contact times, suitability for wide ranges of concentration including zero coverage, and the convenience of a rapid and simple technique.

Gas chromatography offers a unique mean of studying thermodynamic parameters of adsorption, and adsorption isotherms at very low surface coverage, a region of concentrations very important in characterizing the structure of the solid surface. However, gas chromatographic techniques can be extended to higher concentrations as well. Physico-

*Corresponding author. Tel.: +30-61-997-109/997-144; fax: +30-61-997-118/997-110.

E-mail address: gkaraisk@upatras.gr (G. Karaiskakis)

0021-9673/99/$ – see front matter
PII: S0021-9673(99)00149-1

chemical measurements for the sorption processes have been described in detail [1,2].

There is a relatively new gas chromatographic methodology allowing the determination of adsorption/desorption rate and equilibrium constants, and rate constants in catalytic reactions, all these simultaneously in a single gas chromatographic experiment. The method is based on reversed-flow gas chromatography (RFGC) [3,4]. The technique reverses the direction of flow of the carrier gas, usually for a short time interval. When the carrier gas contains other gases at certain concentrations, recorded by the detector system, the flow reversals create perturbations on the chromatographic elution curve, having the form of narrow and symmetrical extra peaks (sample peaks). If the concentration of a constituent in the flowing gas depends on a rate process taking place within a gaseous diffusion column containing a solid bed, then, by repeatedly reversing the flow, one performs a repeated sampling of this rate process. Using suitable mathematical analysis, equations are derived by means of which the rate coefficients of the slow processes responsible for the sample peaks are determined.

RFGC has been used to determine adsorption equilibrium constants [5], gas diffusion coefficients in binary and ternary mixtures [6,7], activity coefficients [8], mass transfer coefficients on solids and liquids [9–13], solubility and interaction parameters in polymer–solvent systems [14], molecular diameters and critical volumes in gases [15], Lennard–Jones parameters [16], as well as rate constants and activation parameters [17–20]. Conversions of the reactants into products for various important surface-catalysed reactions have also been determined by RFGC [17–20].

To investigate the CO oxidation reaction over the Pt–Rh alloy catalysts, the RFGC technique was applied for the sorption study of CO, O_2 and CO_2 on these bimetallic catalysts.

2. Experimental

2.1. Materials

The catalysts used were Pt–Rh bimetallic catalysts (25% Pt+75% Rh and 75% Pt+25% Rh) supported on SiO_2 (3%, w/w), as well as pure Pt supported also on SiO_2 (3%, w/w). All these catalysts were supplied by Dr. Nieuwenhuys at the Leiden University (Leiden, The Netherlands). The method of preparation and the surface characterization of the catalysts using TDS and X-ray photoelectron spectrometry have been presented previously [21,22]. Before use the catalysts were reduced at 628 K for 10 h in flowing hydrogen at a flow-rate of 1.0 $cm^3 s^{-1}$.

CO from Linde (99.97% pure), CO_2 from Matheson Gas Products (99.97% pure) and O_2 from BOC Gases (99.999% pure) were used as adsorbates.

The carrier gas was helium of purity 99.999% from BOC Gases, while the hydrogen used for the reduction of the catalysts was purchased from Linde (99.999% pure).

The chromatographic material was silica gel 80–100 mesh from Supelco.

2.2. Apparatus and procedure

An outline of the experimental arrangement, which has been described in detail elsewhere [3,4,12,13], is given in Fig. 1. The sampling cell consists of the sampling column, $l'+l$ [(38+38) cm×4 mm I.D.] and the diffusion column of length L (117.6 cm×4 mm I.D.). The latter was connected perpendicularly at its lower end to the middle of the column $l'+l$. Both columns, which were accommodated inside the oven 1 of a usual gas chromatograph (Shimadzu 8A), were empty of any material, except for a short length (~1.0 cm) at the upper end of column L, which contained the catalyst (0.09–0.18 g). The end D_1 of the sampling column $l'+l$ was connected, via a six-port valve, to the carrier gas supply, while the other end D_2 was connected to the separation column of length L', which was placed in oven 2 of another gas chromatograph (Pye–Unicam, Series 104). The end of this column was connected to the thermal conductivity detection (TCD) system, as shown in Fig. 1.

The separation column L' (45 cm×4 mm I.D.) had been filled with silica gel 80–100 mesh (7.6 g) for the separation of the adsorbates (CO, O_2 or CO_2) with possible products (e.g. separation of CO from CO_2 resulted from the CO disproportionation).

Before measurements, the whole system was

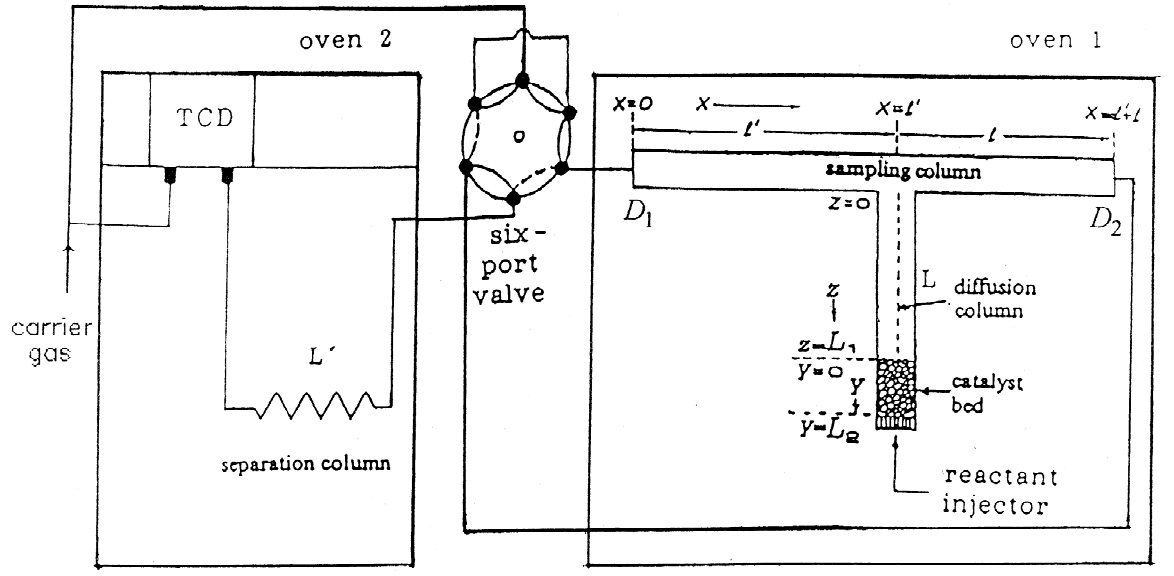

Fig. 1. Experimental set-up of the reversed-flow gas chromatography technique for studying the adsorption of carbon monoxide, oxygen and carbon dioxide on Pt–Rh alloy catalysts.

conditioned by heating in situ the catalyst at 743 K and the silica gel at 423 K both for 20 h, under carrier gas helium flow. Some preliminary injections of the adsorbates CO, O_2 and CO_2 were made to stabilize the catalysts, and then, with the carrier gas flowing in direction from D_1 to D_2 (cf. Fig. 1) with a flow-rate of 1.0 cm^3 s^{-1}, 1 cm^3 of CO, O_2 or CO_2 under atmospheric pressure was rapidly introduced with a gas-tight syringe at the top of the diffusion column *L*. In about 10–20 min a continuous concentration–time curve, increasing initially and then decreasing after a maximum, was recorded due to both the adsorbate and the possible product. During this time period, reversals of the carrier gas flow-direction for 5 s were made, and then the gas was again turned to its original direction, by simply turning the six-port valve from one position to the other, and vice versa. Because the reversal duration was less than the gas hold-up time in the empty columns *l* and *l′*, one (or two—in case the adsorbate reacts on the catalyst surface and gives a product—) symmetrical ''sample peak'' followed each restoration of the gas flow to its original direction [3,4]. An example is given in Fig. 2. The first peak belongs to the adsorbate CO and the other to the product CO_2, which results from the CO disproportionation reaction. The above flow reversal procedure was repeated many times at each temperature, giving rise to one (for the O_2 and CO_2 adsorption) or two (for the CO adsorption) series of sample peaks, each peak or pair (one for the CO and one for the CO_2) of peaks corresponding to a different time from the adsorbate injection.

The pressure drop along the whole system was negligible. The working temperature was 553–748 K for the catalyst bed, and it was kept constant at 358 K for the separation material. The volumetric carrier gas flow-rate at ambient temperature was 1.0 cm^3 s^{-1}.

3. Theory

The height *h* of the sample peaks, obtained by repeated flow reversals, is proportional to the concentration $c(l', t)$ at the point $x=l'$ and at time *t* [23]:

$$h^{1/M} = gc(l', t) \quad (1)$$

M being the response factor of the detector, which can be determined as described elsewhere [24], and *g*

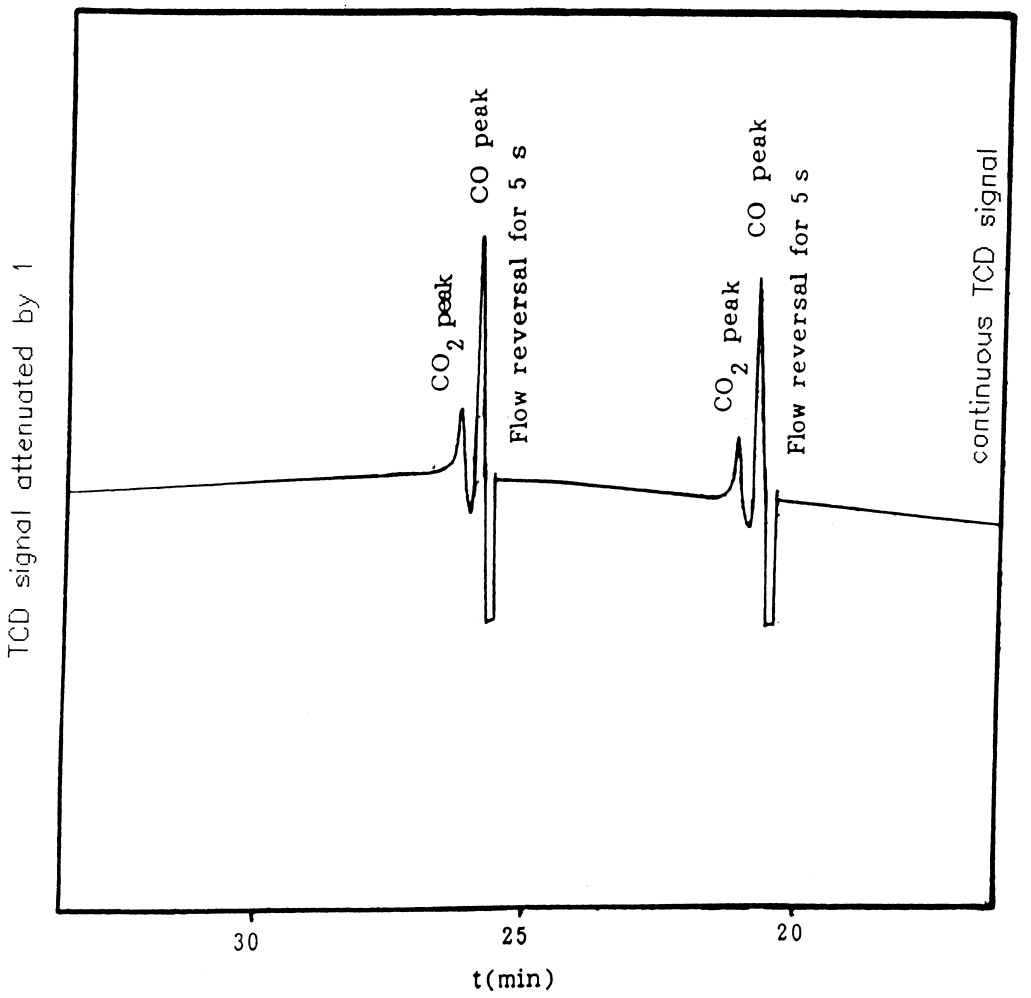

Fig. 2. Reversed-flow gas chromatogram showing two sample peaks for the adsorbate CO (the first peak) and the product CO_2 (the second peak) resulted from the dissociative adsorption of CO on the catalyst 25% Pt+75% Rh (T=673 K).

the proportionality constant (usually assumed unity for convenience).

The mathematical equation describing the ''diffusion band'' (if ln h is plotted against t) of each adsorbate (CO, O_2 and CO_2) in the presence of catalyst is the following [23]:

$$h^{1/M} = A_1 \exp(B_1 t) + A_2 \exp(B_2 t) \quad (2)$$

where:

$$A_1 = N \cdot \left(1 + \frac{Z}{Y}\right) \quad (3)$$

$$A_2 = N \cdot \left(1 - \frac{Z}{Y}\right) \quad (4)$$

$$B_1 = -\frac{X+Y}{2} \quad (5)$$

$$B_2 = -\frac{X-Y}{2} \quad (6)$$

$$N = \frac{gma_1}{2(1+V_1)\dot{V}} \quad (7)$$

while the auxiliary parameters X, Y and Z are defined by the relations [23]:

$$X = \frac{a_1}{1+V_1} + \frac{V_1 k_1}{1+V_1} + k_{-1} + k_2 \quad (8)$$

$$\frac{X^2 - Y^2}{4} = \frac{a_1(k_{-1}+k_2)}{1+V_1} + \frac{V_1 k_1 k_2}{1+V_1} \quad (9)$$

$$Z = X - 2(k_{-1} + k_2) \quad (10)$$

where:

$$a_1 = \frac{2D_1}{L_1^2} \quad (11)$$

$$a_2 = \frac{2D_2}{L_2^2} \quad (12)$$

$$V_1 = 2 \cdot \frac{V'_{G(empty)}\varepsilon}{V_G} + \frac{a_1}{a_2} \quad (13)$$

In the last equations V_G and $V'_{G(empty)}$ denote gaseous volumes of empty sections L_1 and L_2, respectively, in m^3 (cf. Fig. 1), k_1 and k_{-1} are rate constants for adsorption and desorption, respectively, in s^{-1}, k_2 is the first-order rate constant for a possible surface reaction in s^{-1}, ε is the external porosity of catalyst bed, m is the amount of the adsorbate injected in mol, and is the volumetric flow-rate of carrier gas in $m^3\ s^{-1}$. The quantities a_1 and a_2 are called diffusion parameters as they depend on the diffusion coefficients D_1 ($m^2\ s^{-1}$) and D_2 ($m^2\ s^{-1}$), respectively. Their dimensions are s^{-1}.

By using a nonlinear regression analysis computer program, the two preexponential factors A_1 and A_2 of Eq. (2), and the two exponential coefficients of time B_1 and B_2 can be calculated from the experimental pairs of values of h and t (h is the height in arbitrary units of the sample peaks and t the respective times, when reversal of carrier gas-flow was made). Such a program in GW-BASIC has already been published [25].

The rate constants for adsorption (k_1) and desorption (k_{-1}), and the rate constants for a possible surface reaction (k_2) can be calculated as follows:

By adding the two exponential coefficients B_1 and B_2 of Eq. (2), we find the value of X, while by subtracting them, we obtain the value of Y:

$$B_1 + B_2 = \left(-\frac{X+Y}{2}\right) + \left(-\frac{X-Y}{2}\right) = -X \quad (14)$$

$$B_1 - B_2 = \left(-\frac{X+Y}{2}\right) - \left(-\frac{X-Y}{2}\right) = -Y \quad (15)$$

From the ratio of the two preexponential factors A_1 and A_2 ($\lambda = A_1/A_2$) the value of Z is found:

$$Z = \frac{1-\lambda}{1+\lambda} \cdot Y \quad (16)$$

The values of the auxiliary parameters X, Y and Z, so found, are now used in conjunction with Eqs. (8), (9) and (10), to calculate the rate constants k_1, k_{-1} and k_2, by means of the relations:

Table 1
Rate constants for adsorption (k_1), desorption (k_{-1}) and disproportionation reaction (k_2) of carbon monoxide on Pt–Rh catalysts determined by the reversed-flow gas chromatography technique at various temperatures

Catalyst	T (°C)	k_1 ($10^{-1}\ s^{-1}$)	k_{-1} ($10^{-4}\ s^{-1}$)	k_2 ($10^{-4}\ s^{-1}$)
100% Pt	282	1.33	6.09	2.80
	301	1.41	6.48	2.90
	323	1.59	6.76	3.63
	343	1.63	6.85	4.04
	361	1.86	7.35	4.13
	370	1.84	7.63	3.78
	385	1.83	7.82	3.98
	400	1.98	8.23	4.00
	419	2.13	8.74	4.15
	435	2.27	9.29	4.58
	451	2.68	9.62	4.53
75% Pt+25% Rh	279	0.91	6.33	1.86
	302	1.04	6.57	2.03
	321	–	6.86	–
	340	1.38	7.34	2.28
	361	–	7.97	–
	380	1.16	8.18	2.18
	401	1.36	8.88	2.31
	436	1.52	9.50	2.45
25% Pt+75% Rh	280	0.76	2.59	5.21
	301	0.73	2.29	5.76
	326	0.94	3.70	5.34
	351	1.21	4.80	5.36
	376	1.39	6.19	4.72
	405	1.83	7.26	–
	420	2.35	8.44	3.84
	464	2.64	–	3.90

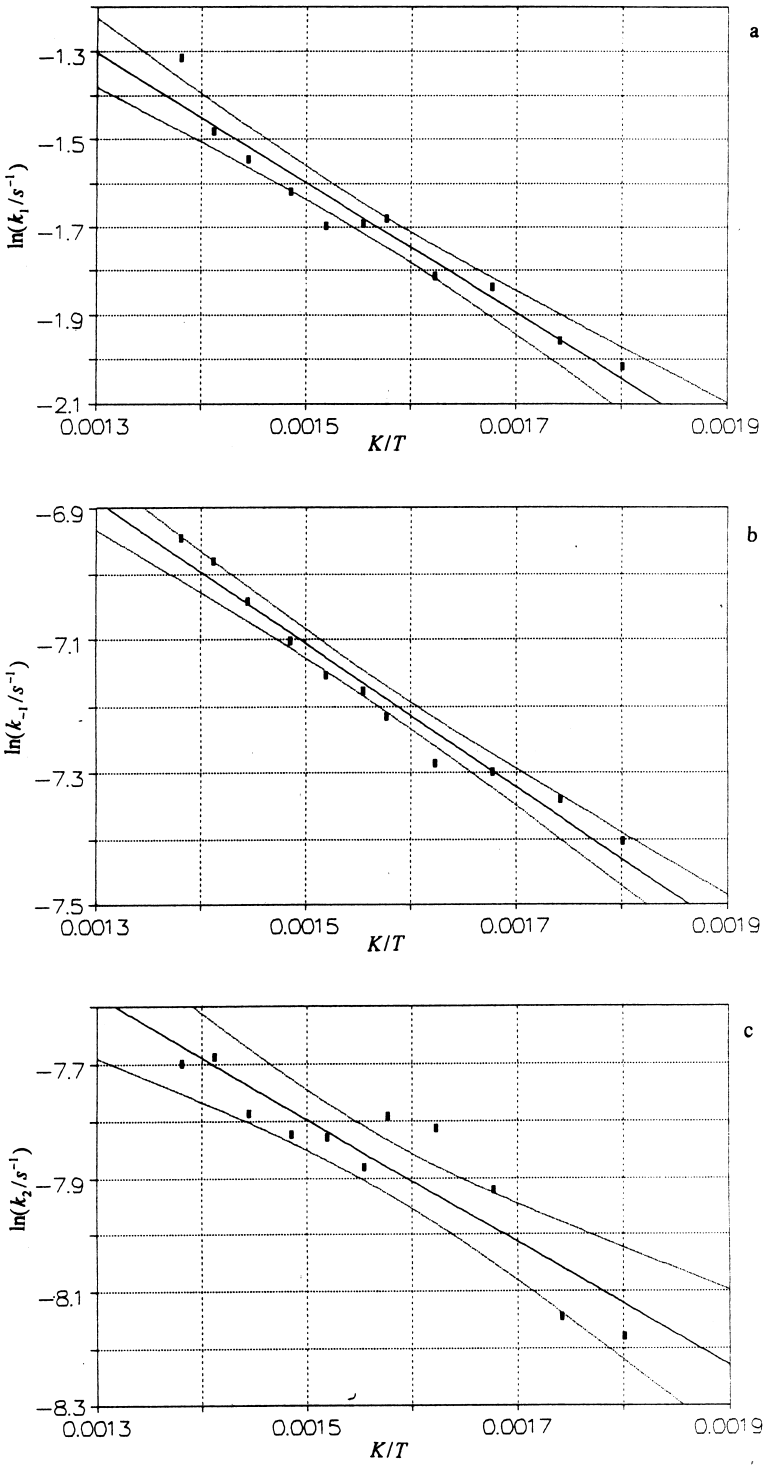

Fig. 3. Arrhenius plots with their 95% confidence limits for the CO adsorption (a), desorption (b) and disproportionation reaction (c) over the pure Pt catalyst.

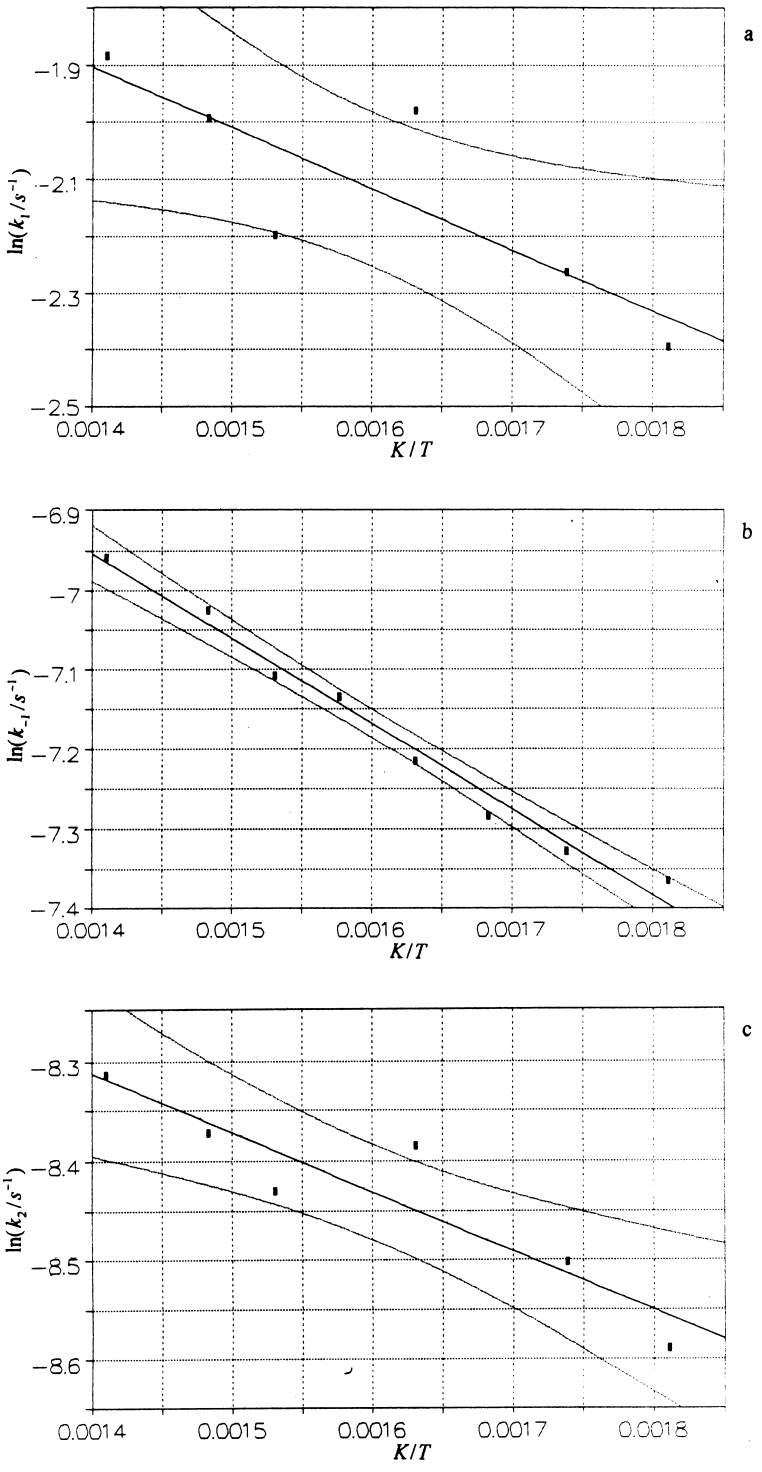

Fig. 4. Arrhenius plots with their 95% confidence limits for the CO adsorption (a), desorption (b) and disproportionation reaction (c) over the catalyst 75% Pt+25% Rh.

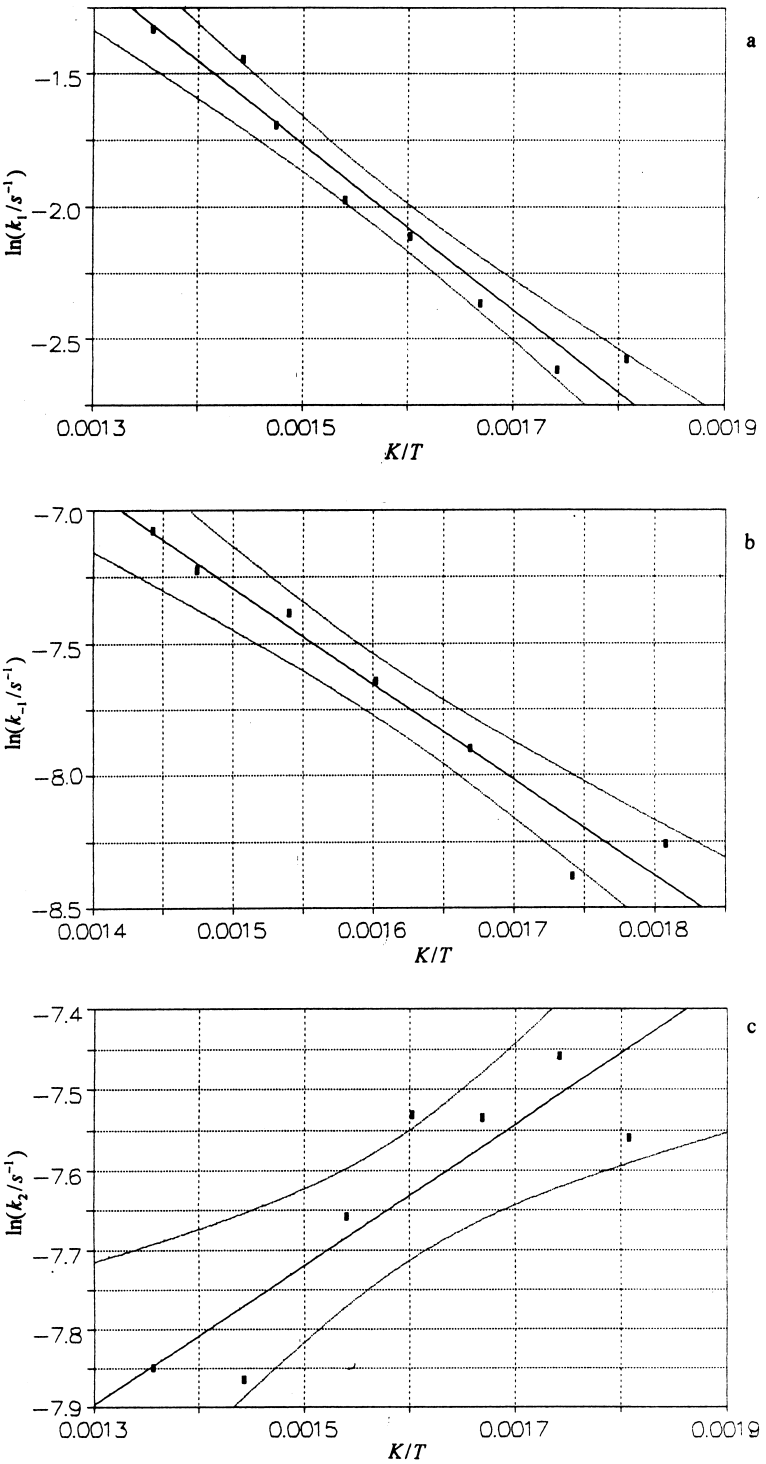

Fig. 5. Arrhenius plots with their 95% confidence limits for the CO adsorption (a), desorption (b) and disproportionation reaction (c) over the catalyst 25% Pt+75% Rh.

$$k_1 = \frac{(X+Z)(1+V_1) - 2a_1}{2V_1} \quad (17)$$

$$k_2 = \frac{(X^2 - Y^2)(1+V_1) - 2a_1(X-Z)}{2(X+Z)(1+V_1) - 4a_1} \quad (18)$$

$$k_{-1} = \frac{X-Z}{2} - k_2 \quad (19)$$

When $k_2 = 0$ (which means that the adsorbate does not react on the catalyst surface), the auxiliary parameters X, Y and Z are given by the relations:

$$X = \frac{a_1}{1+V_1} + \frac{V_1 k_1}{1+V_1} + k_{-1} \quad (20)$$

$$\frac{X^2 - Y^2}{4} = \frac{a_1 k_{-1}}{1+V_1} \quad (21)$$

$$Z = X - 2k_{-1} \quad (22)$$

The values of X, Y and Z, found from the last equations by the procedure described previously, are now used in conjunction with Eqs. (17) and (19) to calculate the rate constants k_1 and k_{-1}.

The last equations show that, except for X, Y and Z, calculated by means of Eqs. (14), (15), (16), (20), (21) and (22), the diffusion parameters a_1 and a_2 [cf. Eqs. (11) and (12)], and the parameter V_1 defined by Eq. (13) are required in the calculation above. The a_1 and a_2 are easily calculated from the diffusion

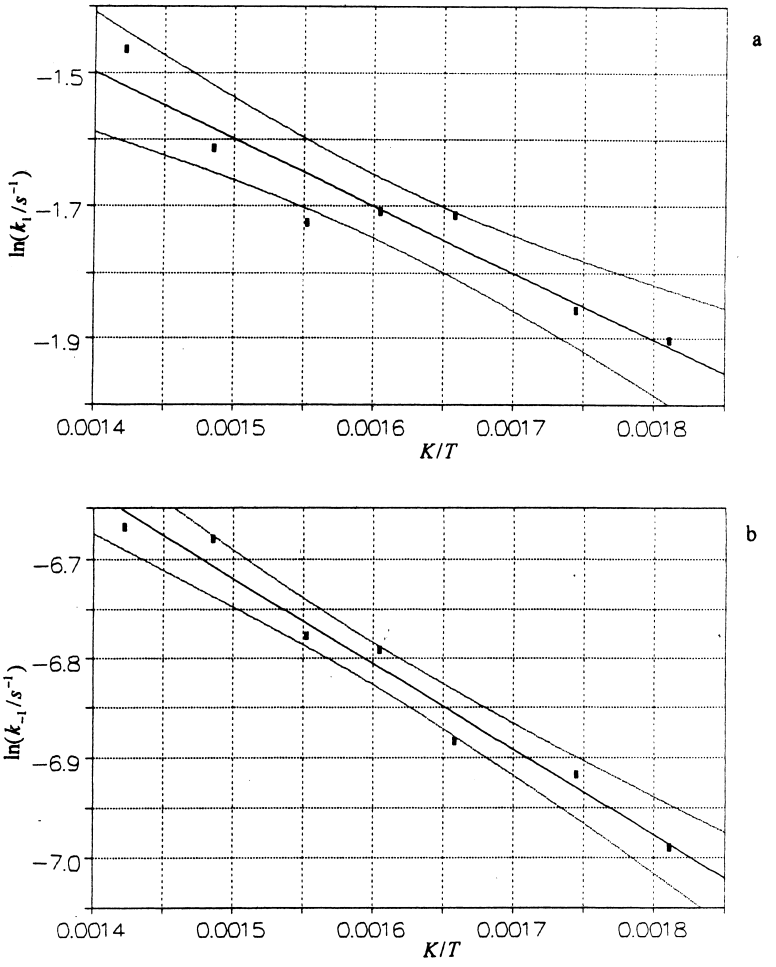

Fig. 6. Arrhenius plots with their 95% confidence limits for the adsorption (a) and desorption (b) of oxygen on the pure Pt catalyst.

coefficients D_1 and D_2 at temperatures T_1 and T_2, respectively, determined as described elsewhere [6,7]. The parameter V_1 is calculated from Eq. (13), while the external porosity ε of the catalyst bed can be found as described previously [19].

Thus, the RFGC technique can be applied to the adsorption and desorption of adsorbate molecules regardless of the fact that these may react, i.e., both associative ($k_2=0$) and dissociative ($k_2\neq 0$) adsorption can be studied.

4. Results and discussion

Following the procedure described in the Experimental Section, we found that each flow reversal gives two sample peaks for the adsorption of CO on the catalysts used (cf. Fig. 2), and one sample peak for the adsorption of O_2 and CO_2 on the same catalysts. The latter indicates a dissociative adsorption of CO on all the catalysts used. X-ray defraction analysis of the catalysts at the end of the experiments has shown the deposition of carbon on the catalytic surface and verified the disproportionation of CO.

Although it is well established in the literature [21,26] that the primary reaction pathway for the oxidation of CO on noble metals is a surface reaction between adsorbed CO and adsorbed atomic O, the present results, in accordance with other previous works [27–29], suggest a CO dissociation followed

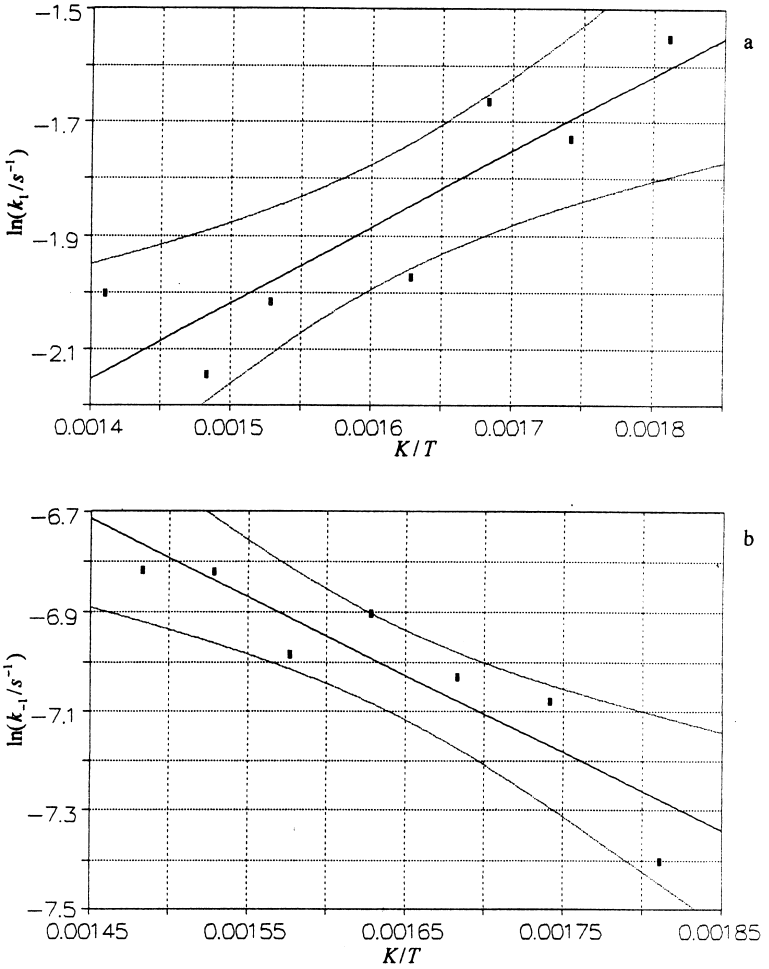

Fig. 7. Arrhenius plots with their 95% confidence limits for the adsorption (a) and desorption (b) of oxygen on the catalyst 75% Pt+25% Rh.

by reaction of adsorbed CO molecules and O adatoms, as follows:

$$3CO(g) + 3* \leftrightarrow 3CO(ads)$$

$$CO(ads) + * \rightarrow C(ads) + O(ads)$$

$$O_2(g) + 2* \leftrightarrow 2O(ads)$$

$$3CO(ads) + 3O(ads) \rightarrow 3CO_2(g) + 6*$$

where [*] denotes the concentration of vacant active sites.

The experimental data for the adsorption of CO, which have been analysed by the procedure described in the Theoretical Section, lead to the determination of rate constants for the CO adsorption (k_1) and desorption (k_{-1}), as well as for the CO disproportionation reaction (k_2). On the other hand the adsorption of O_2 and CO_2 leads only to the determination of rate constants for the adsorption (k_1) and desorption (k_{-1}), as the adsorbates do not react on the catalyst surface and $k_2 = 0$.

The rate constants for adsorption (k_1) and desorption (k_{-1}) of CO on and from the catalysts used, and the rate constants for the disproportionation reaction of CO (k_2) over the same catalysts as a function of temperature, are compiled in Table 1. From the values of k_1, k_{-1} and k_2 for the adsorption of CO given in Table 1 and their variation with temperature shown in Figs. 3–5 in the form of ln k vs. $1/T$, the following conclusions can be drawn:

1. The adsorption rate constants found in the present work by the RFGC technique are very close to those determined experimentally by the frequency response method [30] for the adsorption of CO on Pt/SiO_2. The latter shows that reversed flow gas chromatography can be applied with simplicity and accuracy for the study of the CO adsorption on Pt–Rh alloy catalysts.
2. In all catalysts, the k_1 and k_{-1} values increase

Table 2
Rate constants for adsorption (k_1), and desorption (k_{-1}) of oxygen on Pt–Rh catalysts determined by reversed-flow gas chromatography at various temperatures

Catalyst	T (°C)	k_1 (10^{-1} s^{-1})	k_{-1} (10^{-4} s^{-1})
100% Pt	279	1.49	9.20
	300	1.56	9.90
	330	1.80	10.24
	350	1.81	11.22
	371	1.78	11.39
	400	1.99	12.55
	430	2.31	12.69
75% Pt+25% Rh	279	2.12	6.09
	301	1.77	8.41
	321	1.89	8.84
	341	1.39	10.02
	361	–	9.24
	381	1.33	10.90
	401	1.17	10.93
	436	1.35	–
25% Pt+75% Rh	280	0.91	8.52
	301	1.08	8.95
	325	1.09	9.50
	350	1.27	10.26
	375	1.33	10.88
	400	1.73	12.06
	425	2.01	12.70
	450	2.45	14.18
	472	2.78	–

Table 3
Rate constants for adsorption (k_1), and desorption (k_{-1}) of carbon dioxide on Pt–Rh catalysts determined by reversed-flow gas chromatography at various temperatures

Catalyst	T (°C)	k_1 (10^{-1} s^{-1})	k_{-1} (10^{-4} s^{-1})
100% Pt	280	1.17	7.75
	301	–	7.61
	325	1.50	8.69
	350	–	9.36
	371	1.58	9.55
	375	1.53	10.61
	400	1.53	10.86
	425	1.56	11.83
	450	1.76	11.37
75% Pt+25% Rh	280	1.01	7.35
	301	0.97	7.71
	321	0.91	7.79
	361	1.01	8.51
	381	1.21	9.05
	401	1.34	9.73
	435	1.67	10.22
25% Pt+75% Rh	280	1.32	6.84
	301	–	7.74
	325	1.59	8.28
	350	1.52	8.50
	375	1.59	8.99
	400	1.63	9.66
	425	1.83	10.87
	450	1.87	11.48

with increasing temperature, according to Arrhenius equation.

3. The k_1 values are higher for the pure Pt catalyst indicating that CO is adsorbed more strongly on the Pt catalyst than on the Pt–Rh bimetallic catalysts. Similar results for the same catalysts by using different techniques were also reported previously [21].
4. The k_{-1} values are about the same for the bimetallic catalysts, but are lower for the pure Pt catalyst at least at low temperatures.
5. The k_2 values increase with increasing temperature for the catalysts 100% Pt and 75% Pt+25% Rh. The anomalous observation of the k_2 decrease with increasing temperature for the catalyst 25% Pt+75% Rh can be explained as follows: The calculated rate constants for the disproportionation reaction of CO (k_2) are the apparent ones. These are related to the true k_2 values, k_2^{true}, via the equation: $k_2^{\text{true}} = k_2/K$, where K is the equilibrium constant for the disproportionation reaction (the Boudouard reaction) $2CO \leftrightarrow C + CO_2$. It is well established in the literature [29,31] that the equilibrium constant K for the disproportionation reaction of CO over noble metals decreases drastically with temperature due to the fact that at low temperatures the CO disproportionation is kinetically controlled, while at higher tempera-

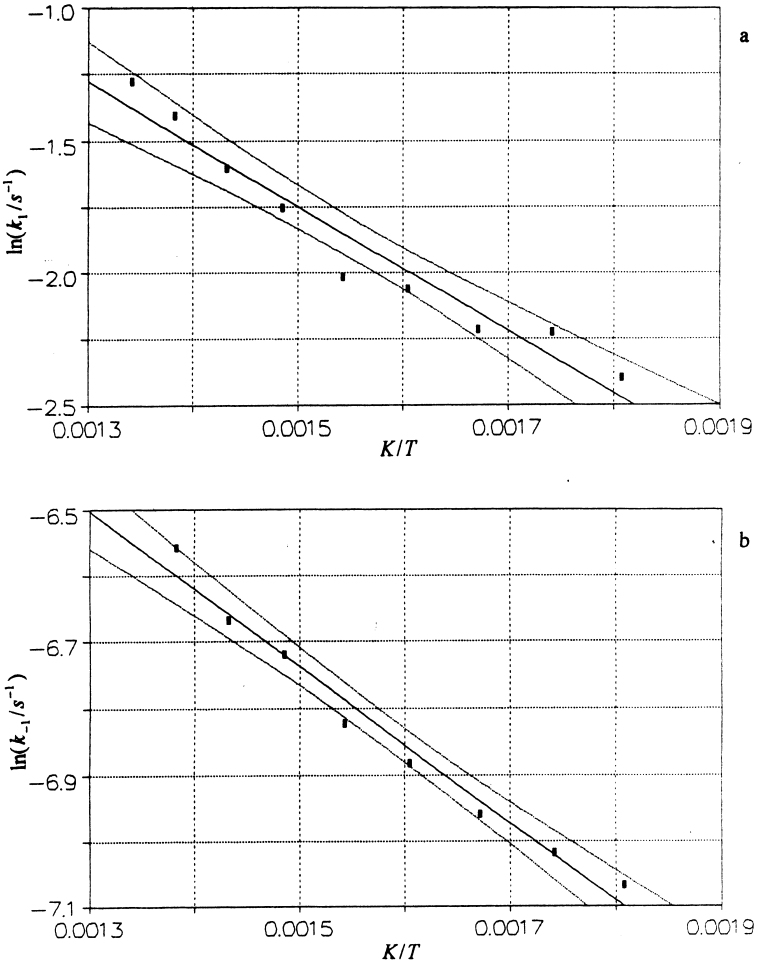

Fig. 8. Arrhenius plots with their 95% confidence limits for the adsorption (a) and desorption (b) of oxygen on the catalyst 25% Pt+75% Rh.

tures equilibrium controls the product composition. Thus, a small decrease of the k_2 value with temperature, accompanied by a higher decrease of the equilibrium constant K, leads to an increase in the true rate constant with temperature, as the theory predicts. The finding that this anomalous behaviour was observed only in the Rh-rich catalyst (25% Pt+75% Rh) can be explained by the fact that, as is well known in the literature [26,32–34] and the k_2 values show, this catalyst is the most active for the CO disproportionation reaction.

From the rate constants k_1 and k_{-1} for the adsorption of O_2 on the catalysts used, which are summarized in Table 2, and their variation with temperature, which is shown in Figs. 6–8 in the form of ln k vs. $1/T$, it is concluded that while the k_{-1} values increase with temperature for all catalysts, the k_1 values increase with increasing temperature for the catalysts 100% Pt and 25% Pt+75% Rh, while decrease with increasing temperature for the catalyst 75% Pt+25% Rh. The latter, which has been also observed previously [21], can be attributed to the following reason: The Pt surface concentration in the Pt-rich catalyst, compared to the Rh surface concentration, according to the surface phonon softening model [21], becomes larger with rising temperature. Considering that the Pt surface in the Pt–Rh alloy catalysts is predominantly covered with CO, while the Rh surface strongly adsorbs O_2, the adsorption of

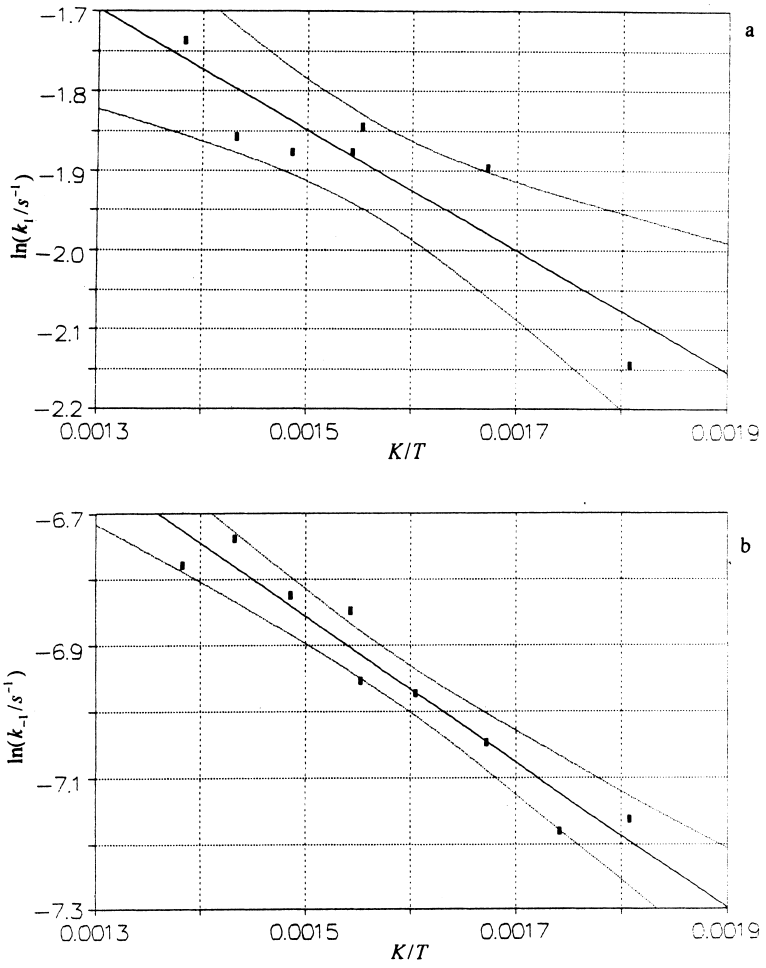

Fig. 9. Arrhenius plots with their 95% confidence limits for the adsorption (a) and desorption (b) of carbon dioxide on the pure Pt catalyst.

O_2 on the Pt-rich catalyst decreases with increasing temperature.

As Table 3 and Figs. 9–11 show the adsorption of CO_2 is rather similar on all the catalysts used, although the k_1 values for the same temperature vary slightly with the catalyst Pt content as follows:

$$k_1(75\%\ \text{Pt} + 25\%\ \text{Rh}) < k_1\ (100\%\ \text{Pt}) < k_1(25\%\ \text{Pt} + 75\%\ \text{Rh})$$

The k_1 and k_{-1} values, as the theory predicts, increase with increasing temperature.

From the variation of ln k_1, ln k_{-1} and ln k_2 with the inverse temperature (cf. Figs. 3–11), activation energies for adsorption, desorption, and disproportionation reaction of CO over Pt–Rh alloys and pure Pt catalysts were determined (cf. Table 4). In the same table the standard errors of the activation energies are compiled as they were calculated by the non-linear form of the Arrhenius equation [35,36]. It must be pointed out that in all figures the regression lines are accompanied with their 95% confidence limits. The values of activation energies obtained for the adsorption and desorption of CO, O_2 and CO_2 on Pt–Rh catalysts, as well as for the disproportionation reaction of CO over the same catalysts are significantly lower than those reported in the literature [37], although some unexpected low values of the

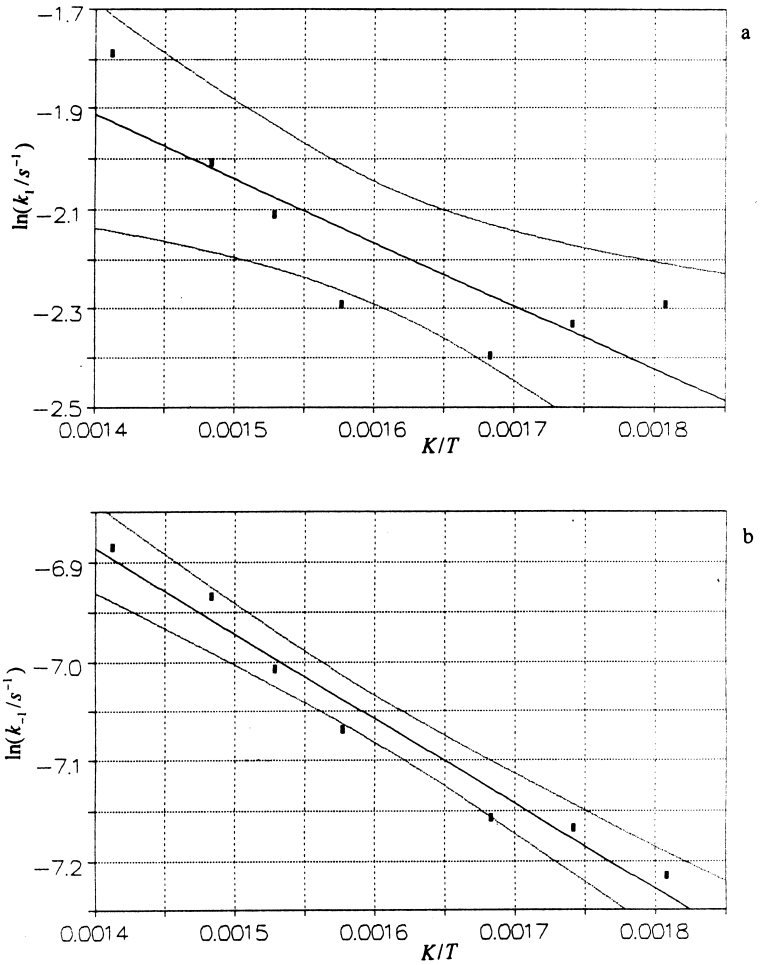

Fig. 10. Arrhenius plots with their 95% confidence limits for the adsorption (a) and desorption (b) of carbon dioxide on the catalyst 75% Pt+25% Rh.

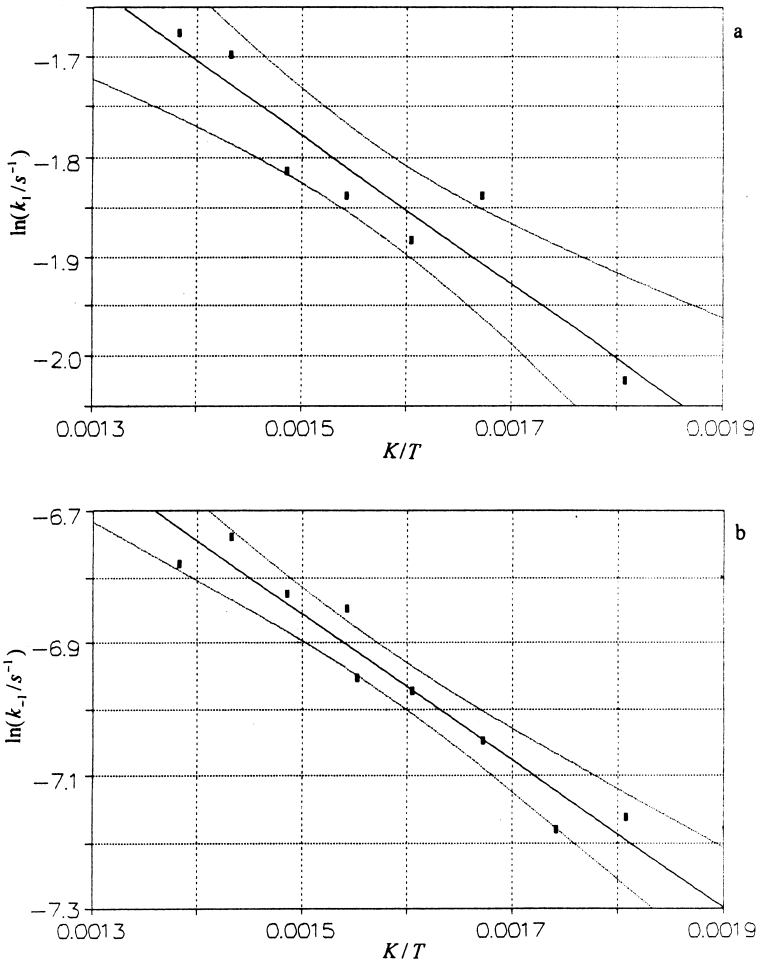

Fig. 11. Arrhenius plots with their 95% confidence limits for the adsorption (a) and desorption (b) of carbon dioxide on the catalyst 25% Pt+25% Rh.

Table 4
Activation energies for adsorption (E_{a1}) and desorption (E_{a-1}) of carbon monoxide, oxygen and carbon dioxide, as well as for the disproportionation reaction (E_{a2}) of carbon monoxide over Pt–Rh catalysts determined by reversed-flow gas chromatography

Catalyst	Adsorbate	E_{a1} (kJ mol^{-1})	E_{a-1} (kJ mol^{-1})	E_{a2} (kJ mol^{-1})
100% Pt	CO	13.1±1.2[a]	9.42±0.57	8.4±1.3
75% Pt+25% Rh		8.7±3.0	9.10±0.45	4.8±1.0
25% Pt+75% Rh		26.9±2.3	30.1±2.1	[b]
100% Pt	O_2	8.7±1.3	7.13±0.57	
75% Pt+25% Rh		[b]	11.8±2.5	
25% Pt+75% Rh		22.4±1.9	10.18±0.65	
100% Pt	CO_2	6.0±1.5	9.07±0.99	
75% Pt+25% Rh		12.6±3.1	7.29±0.59	
25% Pt+75% Rh		6.3±1.1	9.62±0.73	

[a] Standard errors calculated by the nonlinear form of the Arrhenius equation.
[b] Negative values as explained in the text.

apparent activation energy were also observed previously [38] for the oxidation reaction of CO over noble metals. The low values of E_a(E_{a1}, E_{a-1} and E_{a2}) indicate that the found values of rate constants are the apparent ones, therefore making them of trivial importance, in relation to their absolute values. But their variation with temperature or with the catalyst Pt content, considering a process mechanism independent of temperature and catalyst nature, gives useful information about the catalyst activity.

The dependence of E_a (E_{a1}, E_{a-1} and E_{a2}) values on the catalyst Pt content shown in Fig. 12 indicates that the E_{a1} values for the CO adsorption present a minimum for the catalyst containing 75% atom Pt (cf. Fig. 12). It is interested to point out that this catalyst is the most active one for the oxidation reaction of CO [20,26,34], indicating that the CO adsorption rate on the catalyst influences strongly the catalytic activity. Another important conclusion drawn from Fig. 12, which supports the higher catalytic activity of the catalyst 75% Pt+25% Rh, is the fact that the activation energy for the adsorption of CO_2 on the catalysts, has its highest value for the most active catalyst (75% Pt+25% Rh). As far as the activation energy for the O_2 adsorption is concerned, it seems that in the working temperature range O_2 is more easily adsorbed on the pure Pt catalyst than on the bimetallic 25% Pt+75% Rh catalyst, although it has been shown previously [20,26,34] that the bimetallic catalyst compared to pure Pt is more active for both the CO oxidation and disproportionation reactions. Obviously the adsorption of O_2 on the catalysts is not the rate determining step for the above two processes.

The results of Fig. 12 for the desorption of CO and CO_2 from the catalysts illustrate a minimum activation energy for the most active bimetallic catalyst (75% Pt+25% Rh), while those for the desorption of O_2 present a maximum E_{a-1} value on the same catalyst, a result which is in contrast with the catalyst activity. The explanation is the same as previously, because the oxygen's adsorption and desorption is not the rate determining step for the CO oxidation and disproportionation.

The decrease of the activation energy for the CO disproportionation reaction over the 75% Pt+25% Rh bimetallic catalyst (cf. Fig. 12), compared to that over the pure Pt catalyst, can be attributed to the presence of Rh which strongly favours the dissociative adsorption of CO on Pt–Rh bimetallic catalysts [29,34]. The high activity of Rh in CO dissociation can be attributed to creation of new sites at the

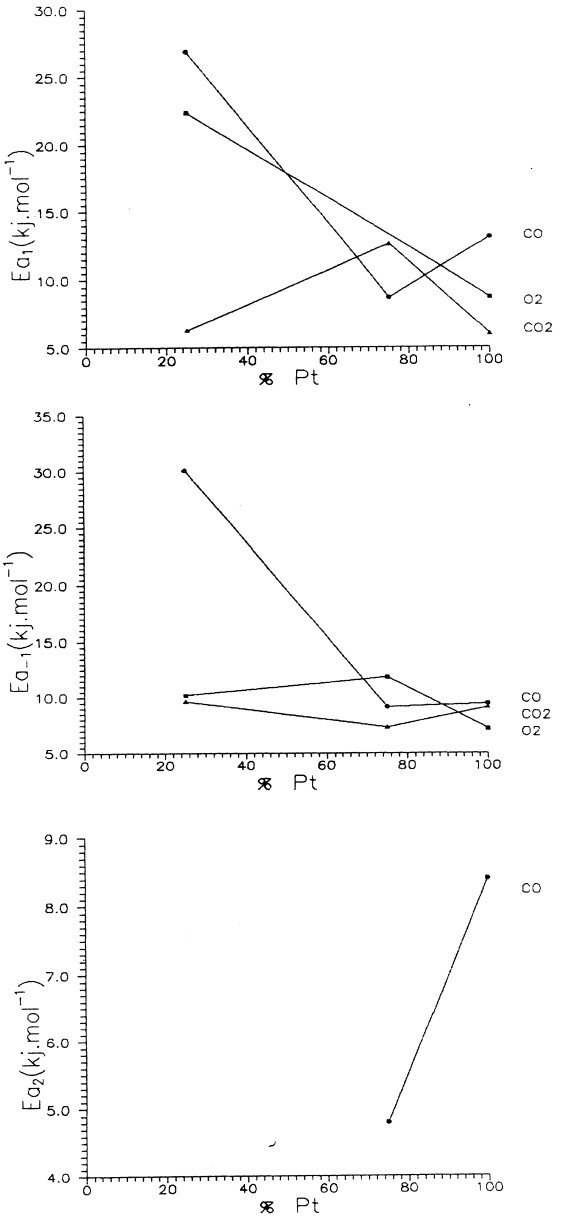

Fig. 12. Variation of activation energy for the adsorption (E_{a1}) and desorption (E_{a-1}) of CO, O_2 and CO_2, as well as for the CO disproportionation reaction (E_{a2}) over Pt–Rh alloy catalysts with the atomic percentage of Pt.

$Rh–SiO_2$ interface, which provides another pathway toward dissociation, assuming that CO can be titled with the O atom toward the catalyst support SiO_2.

As a general conclusion one could say that RFGC can be used with simplicity and accuracy for the study of adsorption of CO, O_2 and CO_2 on Pt–Rh bimetallic catalysts. The results show that the interaction of CO with Pt–Rh alloys supported on SiO_2 leads to its disproportionation and subsequent mechanical deposition of carbon atoms in the form of graphite on the Pt–Rh alloy. This should lead to useful conclusions concerning the mechanism for the CO oxidation and disproportionation reactions.

Acknowledgements

The authors wish to thank Dr. B. Nieuwenhuys at the Leiden University (The Netherlands) for supplying the catalysts, and Mrs. M. Barkoula for the preparation of the typescript.

References

[1] R.J. Laub, R.L. Pecsok, Physicochemical Applications of Gas Chromatography, Wiley, New York, 1978.
[2] J.R. Conder, C.L. Young, Physicochemical Measurement by Gas Chromatography, Wiley, Chichester, 1979.
[3] N.A. Katsanos, Flow Perturbation Gas Chromatography, Marcel Dekker, New York, 1988.
[4] N.A. Katsanos, G. Karaiskakis, Adv. Chromatogr. 24 (1984) 125.
[5] G. Karaiskakis, N.A. Katsanos, A. Niotis, J. Chromatogr. 245 (1982) 21.
[6] N.A. Katsanos, G. Karaiskakis, J. Chromatogr. 237 (1982) 1.
[7] G. Karaiskakis, N.A. Katsanos, A. Niotis, Chromatographia 17 (1983) 310.
[8] N.A. Katsanos, G. Karaiskakis, P. Agathonos, J. Chromatogr. 349 (1986) 369.
[9] G. Karaiskakis, N.A. Katsanos, J. Phys. Chem. 88 (1984) 3674.
[10] N.A. Katsanos, J. Kapolos, Anal. Chem. 61 (1989) 2231.
[11] A. Koliadima, P. Agathonos, G. Karaiskakis, J. Chromatogr. 550 (1991) 171.
[12] D. Gavril, G. Karaiskakis, Instrum. Sci. Technol. 25 (1997) 217.
[13] D. Gavril, G. Karaiskakis, Chromatographia 47 (1998) 63.
[14] P. Agathonos, G. Karaiskakis, J. Appl. Polym. Sci. 37 (1989) 2237.
[15] G. Karaiskakis, A. Niotis, N.A. Katsanos, J. Chromatogr. Sci. 22 (1984) 554.
[16] G. Karaiskakis, J. Chromatogr. Sci. 23 (1985) 360.
[17] N.A. Katsanos, G. Karaiskakis, A. Niotis, J. Catal. 94 (1985) 376.
[18] E. Dalas, N.A. Katsanos, G. Karaiskakis, J. Chem. Soc., Faraday Trans. 1 82 (1986) 2897.
[19] N.A. Katsanos, R. Thede, F. Roubani-Kalantzopoulou, J. Chromatogr. A 795 (1998) 133.
[20] D. Gavril, G. Karaiskakis, submitted for publication.
[21] R.M. Wolf, J. Siera, F.C.M.J.M. van Delft, B.E. Nieuwenhuys, Faraday Discuss. Chem. Soc. 87 (1989) 275.
[22] F.C.M.J.M. van Delft, B.E. Nieuwenhuys, J. Siera, R.M. Wolf, Iron Steel Inst. Jap. Int. 29 (1989) 550.
[23] I. Topalova, A. Niotis, N.A. Katsanos, V. Sotiropoulou, Chromatographia 41 (1995) 227.
[24] V. Sotiropoulou, G.P. Vassilev, N.A. Katsanos, H. Metaxa, F. Roubani-Kalantzopoulou, J. Chem. Soc., Faraday Trans. 1 91 (1995) 485.
[25] A. Niotis, N.A. Katsanos, Chromatographia 34 (1992) 398.
[26] S.H. Oh, J.E. Carpenter, J. Catal. 98 (1986) 178.
[27] D.L. Doering, H. Poppa, J.T. Dickinson, J. Catal. 73 (1982) 104.
[28] S. Ichikawa, H. Poppa, M. Boudart, J. Catal. 91 (1985) 1.
[29] M. Maciejewski, A. Baiker, J. Phys. Chem. 98 (1994) 285.
[30] Y.E. Li, D. Willcox, R.D. Gonzalez, AIChE J. 35 (1989) 423.
[31] G.G. Low, A.T. Bell, J. Catal. 57 (1979) 397.
[32] D.D. Beck, C.J. Carr, J. Catal. 144 (1993) 296.
[33] Z. Hu, F.M. Allen, C.Z. Wan, R.M. Heck, J.J. Steger, R.E. Lakis, C.E. Lyman, J. Catal. 174 (1998) 13.
[34] D. Gavril, A. Koliadima, G. Karaiskakis, Chromatographia, in press.
[35] K. Heberger, S. Kemeny, T. Vidoczy, Int. J. Chem. Kinet. 19 (1987) 171.
[36] C.A. Bennett, N.L. Franklin, Statistical Analysis in Chemistry and the Chemical Industry, Wiley, New York, 1967.
[37] T. Ioannides, A.M. Efstathiou, Z.I. Zhang, X.E. Verykios, J. Catal. 156 (1995) 265.
[38] A. Baiker, M. Maciejewski, S. Tagliaferri, P. Hug, J. Catal. 151 (1995) 407.